

Integrated metabolomic, lipidomic and proteomic analysis define the metabolic changes occurring in curled areas in leaves with leaf peach curl disease

María Lara¹, María Angelina Novello¹, Claudia Bustamante¹, Laura A. Svetaz¹, Camila Goldy¹, Gabriel Valentini², Maria Drincovich¹, Yariv Brotman³, and Alisdair R. Fernie⁴

¹Centro de Estudios Fotosintéticos y Bioquímicos

²Instituto Nacional de Tecnología Agropecuaria

³Tel Aviv University School of Plant Sciences and Food Security

⁴Max-Planck-Institut für Molekulare Pflanzenphysiologie

April 25, 2024

Abstract

Peach Leaf Curl Disease, caused by the fungus *Taphrina deformans*, is characterized by reddish hypertrophic and hyperplastic leaf areas. To comprehend the biochemical imbalances caused by the disease an integrated approach including metabolomics, lipidomics, proteomics and complementary biochemical techniques was undertaken. Symptomatic and asymptomatic areas were dissected from leaves with increasing extension of the disease. A differential metabolic behaviour was identified in symptomatic areas with respect to either asymptomatic areas or healthy leaves. Symptomatic areas showed an altered chloroplastic functioning and composition which includes decrease in the photosynthetic machinery, alteration in plastidic lipids, and decreased starch, carotenoid and chlorophyll biosynthesis. In symptomatic areas, decreases in chloroplast redox-homeostasis proteins and in triacylglycerols double bond index were observed. Proteomic data revealed an up-regulation of phenylpropanoid and mevalonate pathways and down-regulation of the plastidic methylerythritol phosphate route. Amino acid pools were affected, with up-regulation of proteins involved in asparagine synthesis. Curled areas exhibited a metabolic shift towards functioning as a sink tissue importing sugars and producing energy through fermentation and respiration and reductive power via the pentose phosphate route. As the disease progresses, reduced asymptomatic areas and healthy leaves diminishes photosynthates production thereby limiting fruit production and ultimately tree survival.

Hosted file

Novello et al2024.docx available at <https://authorea.com/users/774236/articles/869080-integrated-metabolomic-lipidomic-and-proteomic-analysis-define-the-metabolic-changes-occurring-in-curved-areas-in-leaves-with-leaf-peach-curl-disease>

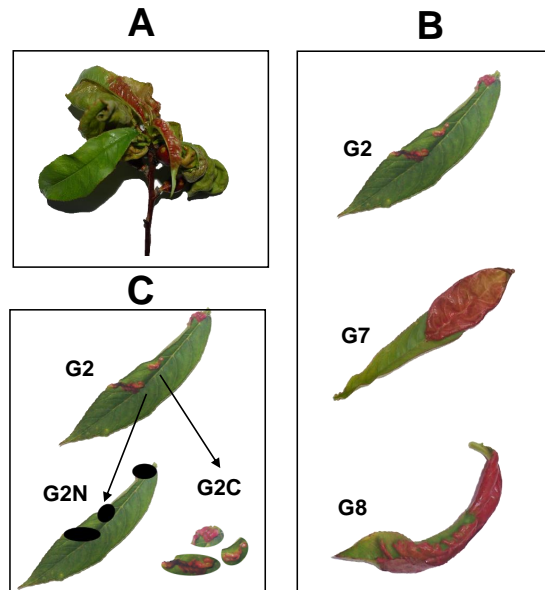


Figure 1. Morphological features of *Prunus persica* leaves showing Peach leaf curl disease. **A.** Image illustrating a typical infected branch. **B.** Leaves with different grades of the disease are shown: G2, grade 2, less than 1 cm of the leaf exhibits symptoms; G7, grade 7, a 50% of the leaf area presents leaf curl and thickening, and G8, grade 8, up to the 75% of the leaf shows typical symptoms of the disease. **C.** Representation of leaf processing. First, leaves were classified as no visible signs of leaf curl (G0) or according to the extent of the disease (G2, G7 or G8). Then, using G2, G7 and G8 leaves, the areas exhibiting curl and thickening (C) were separated from the areas with no symptoms (N).

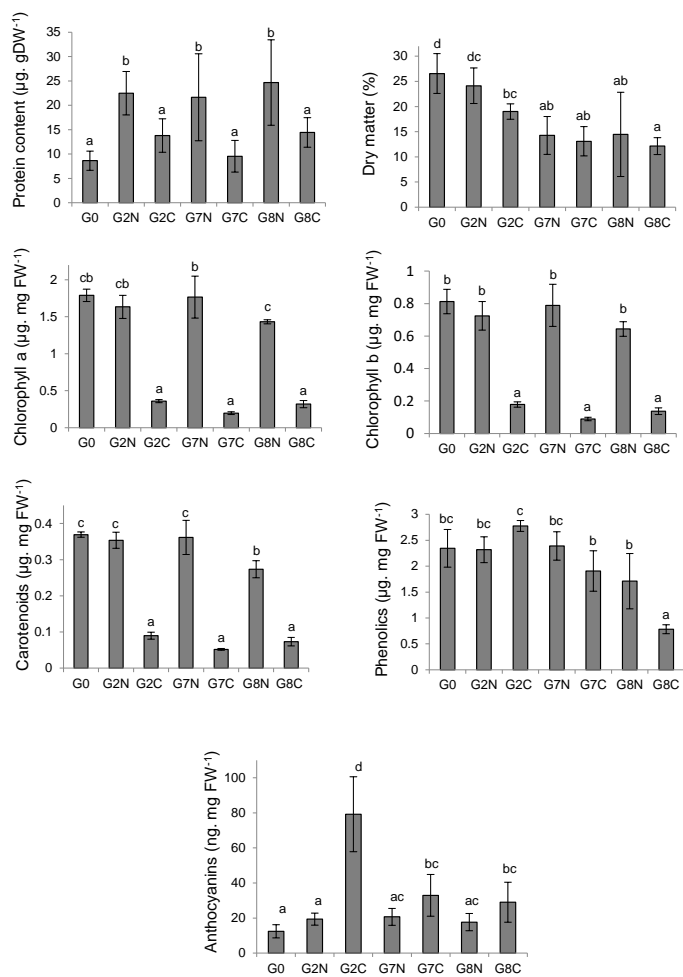


Figure 2. Pigment, proteins and percentage of dry matter quantification. The levels of proteins, chlorophylls, carotenoids, total phenolics and anthocyanins were measured and expressed in a fresh weight (FW) basis. Values represent the mean of at least five independent determinations \pm the SD. The ratio between dry (DW) and fresh weights (FW) \times 100 is the dry matter content (%), $n=15$. Bars with at least one same letter are not statistically different (p -value <0.05).

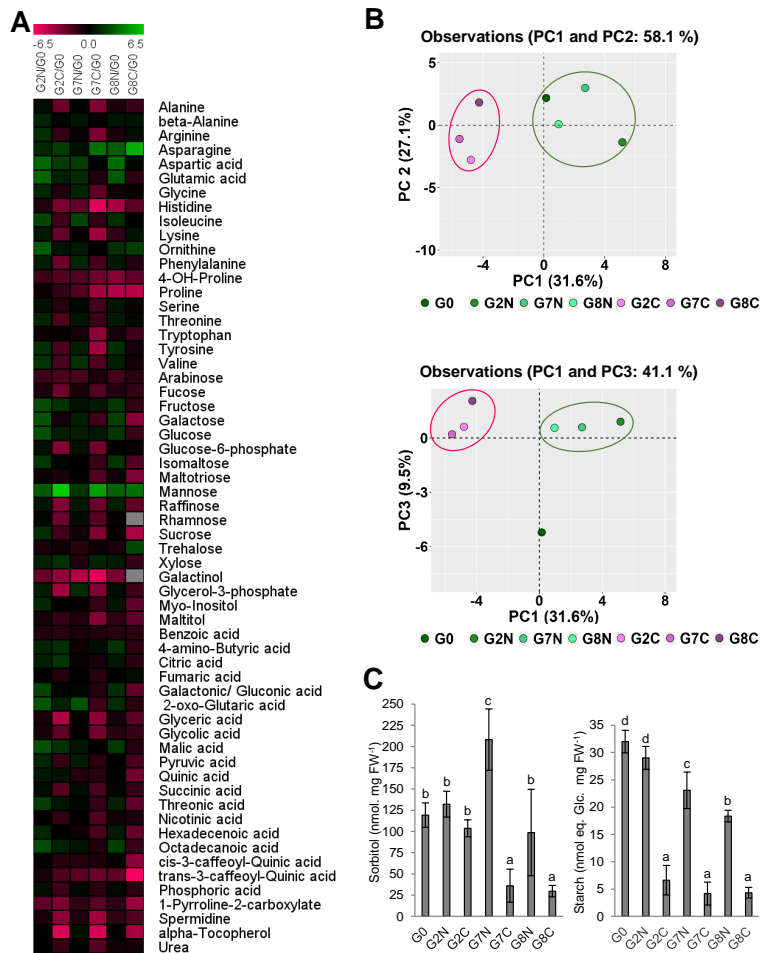


Figure 3. Metabolite profiling in curled and healthy leaves of *P. persica*. **A.** Heat map representing metabolite profiling performed by GC-MS. The heat map displays the relative level of each normalized metabolite to its amount found in G0 leaves (healthy leaves) and expressed as log2. The color scale is shown at the top of the figure and it is proportional to the content of each metabolite. Grey color indicates that the metabolite was not detected, therefore there is not assigned value. At least five biological independent determinations were analyzed for each sample. Relative values for each metabolite peak area \pm SD are displayed in Table S1 and plotted with their corresponding statically analysis in Figure S1. **B.** Principal component analysis (PCA) of metabolite composition by GC-MS. Between parentheses, the variance explained by each component (%) is shown. **C.** Sorbitol and starch contents enzymatically determined. Starch amount is expressed as nmols of glucose released per milligram of fresh weight. Bars with at least one same letter are not significant statically different.

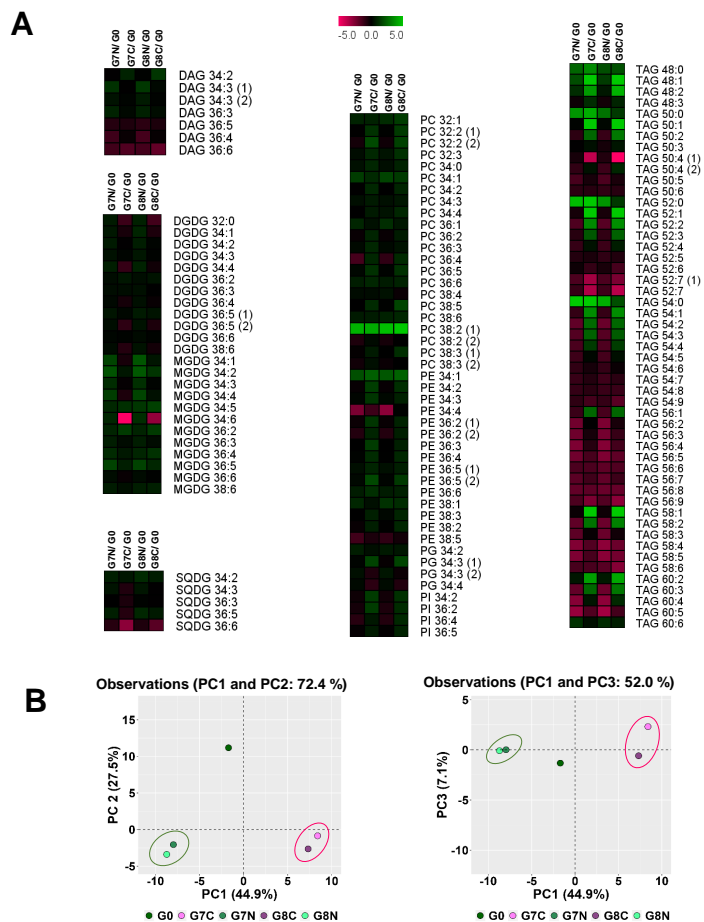


Figure 4. Lipid profiling performed by UPLC-MS. A. Heat map. The heat map displays the relative level of each normalized lipid to its amount found in G0 leaves (no visible symptoms of disease) and expressed as \log_2 . The color scale is shown at the top of the figure and it is proportional to the content of each metabolite. At least five biological independent determinations were analyzed for each sample. Relative values for each metabolite peak area \pm SD are displayed in Table S4 and plotted with their corresponding statistical analysis in Figure S3. Lipid species are annotated based on a C x :y nomenclature where x represents the total carbon number and y is the total number of bound. The numbers between parentheses indicate the presence of different isomers of the same lipid which differ in position of the double bond. For example DGDG36:5 (1) and DGDG36:5 (2). **B.** Principal component analysis (PCA) of lipid profiling. Between parentheses, the variance explained by each component (%) is shown.

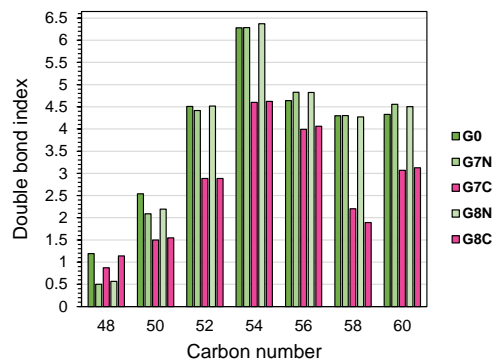


Figure 5. Double bond index of TAGs. TAGs were grouped based on the total carbon number. The DBI was calculated based on the results of lipid profiling generated by UPLC-MS.

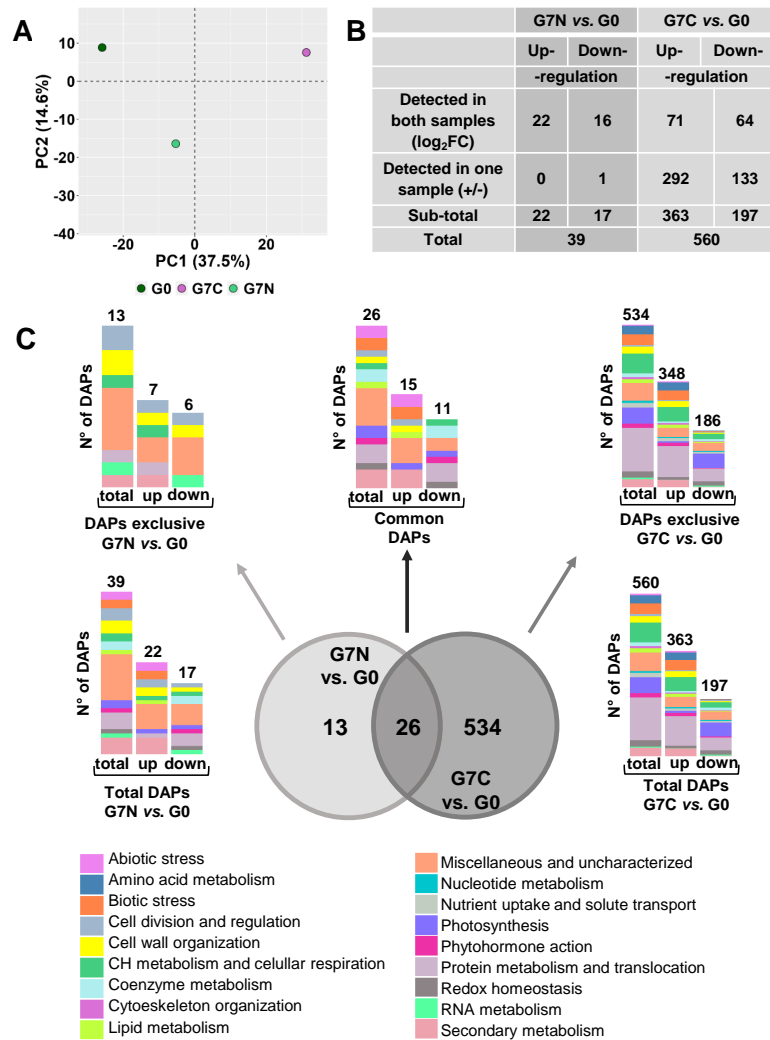


Figure 6. Proteome analysis of PLCD leaves. **A.** Principal component analysis (PCA) of protein profiling. Between parentheses, the variance explained by each component (%) is shown. **B.** Summary of differentially accumulated proteins (DAPs). Up- and down-regulated proteins were computed using Perseus software, p -value < 0.05, 0.05% FDR and q -value < 0.05, DAPs were filtered based on $0.5 < FC < 1.5$. Proteins present in one of the samples of the comparisons but absent in the other sample were also computed as (+) and (-) as depicted in Table S10. **C.** Functional classification of DAPs according to MapMan ontology. Proteins are grouped based on the total number of proteins in the comparison (total), up- or down-regulated proteins. The Venn diagram shows the number of DAPs in the comparisons G7N vs. G0 and G7C vs. G0.

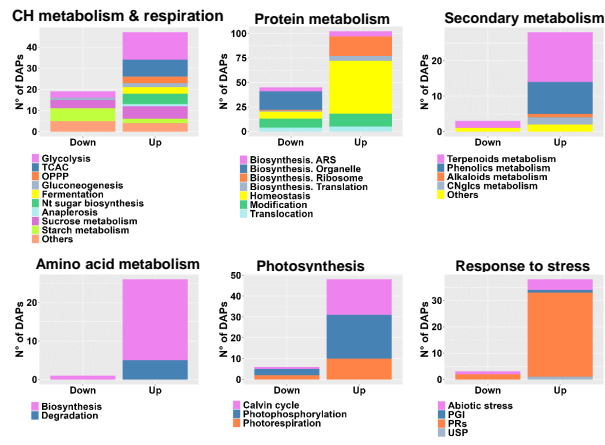


Figure 7. Visualization of proteomic variations in symptomatic areas (G7C) with respect to healthy leaves (G0). Distribution of DAPs in the most represented functional categories by MapMan analysis. Up- and down-regulated proteins are shown separately. Aminoacyl-tRNA synthetase, ARS; BCAA, branched-chain amino acid; Nt, nucleotide; OPPP, oxidative pentose phosphate pathway; PGI, pathogen polygalacturonase inhibitor; TCAC, tricarboxylic acid cycle; USP, universal stress protein.

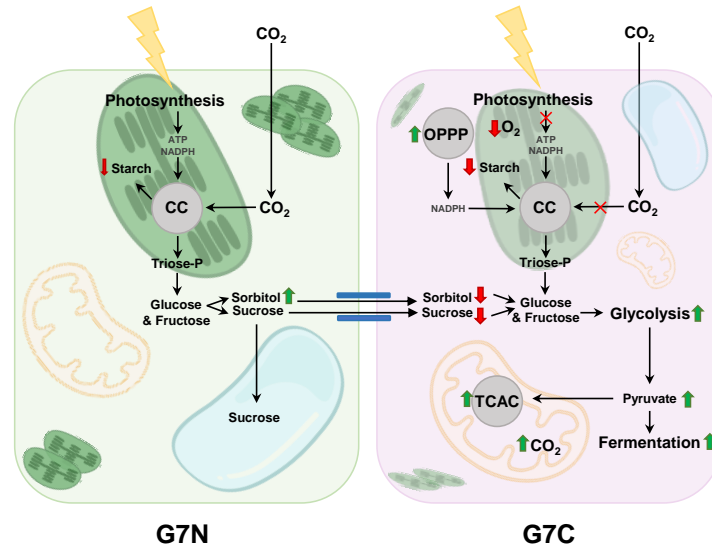


Figure 10. Simplified scheme representing the metabolic changes in cells from asymptomatic and symptomatic areas of leaves with LPC disease. OPPP, pentose phosphate pathway; CC, Calvin Cycle; TCAC, tricarboxylic acid cycle. Plasmodesma is shown in blue. On the right, a typical cell of curled areas is represented. On the left, a mesophyll cell of asymptomatic areas from a leaf with LPCD is shown.

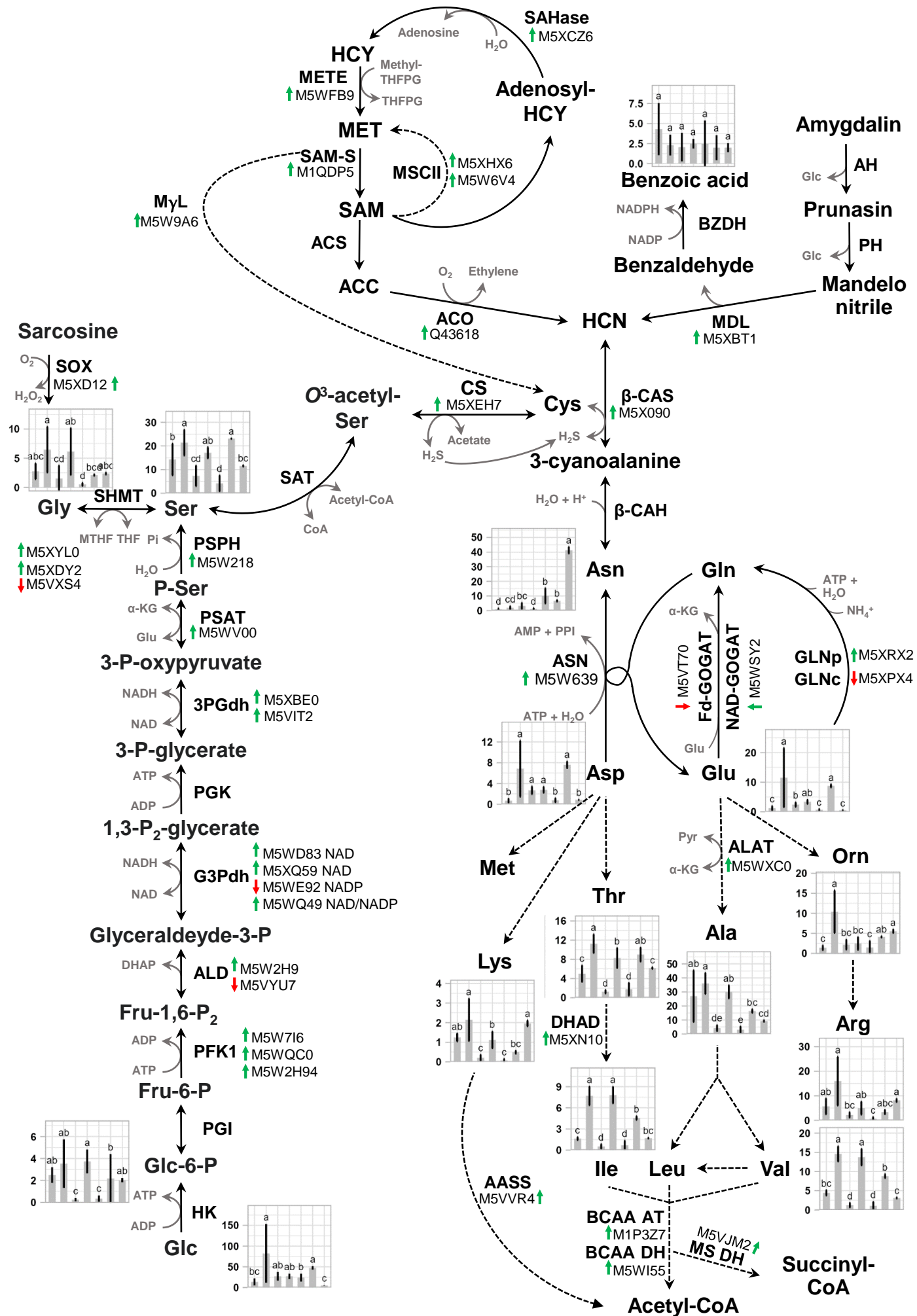


Figure 9. Scheme of amino acid and amino acid-related pathways in *P. persica*. ↑ indicates the increase in the content of the metabolite or protein in G7C with respect to G0. AASS, alpha-amino adipic semialdehyde synthase; ACO, 1-aminocyclopropane-1-carboxylate oxidase; AH, amygdalin hydrolase; ALD, aldolase; ASN, Asparagine synthetase; BCAA AT, branch chain amino acid aminotransferase, BCAA DH, BCCA dehydrogenase; BZDH, benzoic acid dehydrogenase; β -CAS, cyanoalanine synthase; CAH, cyanoalanine hydratase; CS, Cysteine synthase; GLN, Glutamine synthetase; HCY, homocysteine; MSDH, methylmalonate-semialdehyde dehydrogenase; MDL, R-mandelonitrile lyase; MET, 5-methyltetrahydropteroyltriglutamate-homocysteine S-methyltransferase; M γ L, methionine γ lyase, MSCII, L-methionine salvage cycle 2; PFK-1, phosphofructokinase 1; PGK, phosphoglycerate kinase; PH, prunasin hydrolase; PSPH, phosphoserine hydrolase; PSAT, phosphoserine aminotransferase; S-adenosylhomocysteinase, SAHase; SAM-S, S-adenosylmethionine synthase; THFPG, tetrahydropteroyltri-L-glutamate; 3PGDH, 3-phosphoglycerate dehydrogenase.